A scanning hall probe microscope for characterization of micro-magnets and mm-sized magnetic structures

Gorky Shaw, Roman B.G. Kramer, Nora Dempsey, Klaus Hasselbach

A Scanning Hall Probe Microscope For Characterization Of Micro-magnets and mm-Sized Magnetic Structures

Gorky Shaw[1, 2, a)], Roman B. G. Kramer[1], Nora. M. Dempsey[1], and Klaus Hasselbach[1]

[1]*Univ. Grenoble Alpes, CNRS, Institut Néel, 38000, Grenoble, France.*

[2]*Present address: Department of Physics, School of Applied Sciences, Kalinga Institute of Industrial Technology (KIIT), Bhubaneswar, Odisha, India - 751024.*

[a)] Corresponding author: gorky.shawfpy@kiit.ac.in

Abstract. Here we present a scanning Hall probe microscope operated using tuning fork-based force detection technique. A unique feature of the microscope is the use of the same stepper motors for both sample positioning as well as scanning, which allows for a scan range of a few mm, with a scan resolution of 0.1 μm. Scanning at different heights from the sample surface is possible, in a *z* range of 35 mm. A combination of micro-structured Hall probes (of size 1-5 μm) and the tuning fork-based force detection has enabled achieving a minimum probe-sample distance < 2 μm. We discuss the salient features of the microscope and its application for the study of micro-magnet arrays and larger magnetic structures.

INTRODUCTION

Scanning Hall probe microscopy (SHPM) [1-3] stands out among common non-invasive magnetic imaging techniques due to its unique advantages, notably, the possibility of direct quantitative magnetic characterization over large field and temperature ranges. There have been continuous efforts to improve the spatial resolution and scan range [4–7], temperature range [8], and magnetic field resolution [9] of SHPM.

We summarize here the development of a SHPM system built for characterization of arrays of micro-magnets in ambient conditions [10]. In comparison to microscopes presented before [4-9,11], the present system features a combination of several concepts, such as stepper motors for scanning, tuning fork-based contact regulation, and compact electronic circuitry, which contributes to overall system performance. The microscope features a scan range of a few mm, limited by sample topography. The stepper motors offer a minimum step resolution of 0.1 μm (spatial resolution of the magnetic field distribution is limited by the size of the Hall probes as the detected magnetic field is the average field over the active area of the probe) and large *z* range, allowing sample-probe distances from < 2 μm to 35 mm. Micro-structured Hall probes with an active area of 1-5 μm enable large magnetic field detection (fields up to 1 T have been measured) with high field resolution (100 μT, limited by system noise during scanning). In the following sections, firstly the microscope is described and then results showcasing the high resolution and large area scanning capabilities of the microscope are presented.

THE SHPM SYSTEM

The Microscope

Figure 1(a) shows a schematic of the microscope. It consists of two parts. The mobile sample stage consists of a sample holder placed on Micos stepper motors XYZ stage, which allows movement of the sample in all three directions. The travel range of the motors is 50 mm. The minimum step size is 0.1 μm in the X/Y directions, and 0.2 μm in the Z-direction, which are precise enough for the primary purpose our microscope is built for. Hence,

DAE Solid State Physics Symposium 2018
AIP Conf. Proc. 2115, 030210-1–030210-4; https://doi.org/10.1063/1.5113049
Published by AIP Publishing. 978-0-7354-1851-6/$30.00

scanning is performed by the stepper motors themselves, which results in a maximum possible scan range equal to the travel range of the motors. In practice, the range is limited by the sample topography, which restricts the distance over which the desired probe-sample distance regulation (discussed later) can be maintained. With the samples investigated, we have been able to achieve a maximum scan range of 2.5 mm.

The fixed probe stage includes the Hall probe mounted on a commercial quartz tuning fork (resonance frequency $f_R \sim 32.768$ kHz), as shown in Fig. 1(b). This stage also hosts piezoelectric elements for tuning fork excitation and z-regulation, as well as all electrical connections. The tuning fork is mechanically excited via a piezoceramic element (labelled "Excitation piezo" in Fig. 1(a)). The "z-piezo stack" extension piezoelectric element is used for probe-sample distance control (within its extension range of ~ 32 µm) [12,13].

The primary electronics component is a fast lock-in amplifier, Zurich Instruments HF2LI, which provides the excitation signal, and measures the current of the tuning fork. It also provides the Hall excitation current and measures the Hall voltage. It also provides a fast Proportional-Integral-Derivative (PID) control for the z-piezo stack. Custom-built reliable and user-friendly LabVIEW programs for all operations, including data acquisition and analysis, have been developed specifically for the setup.

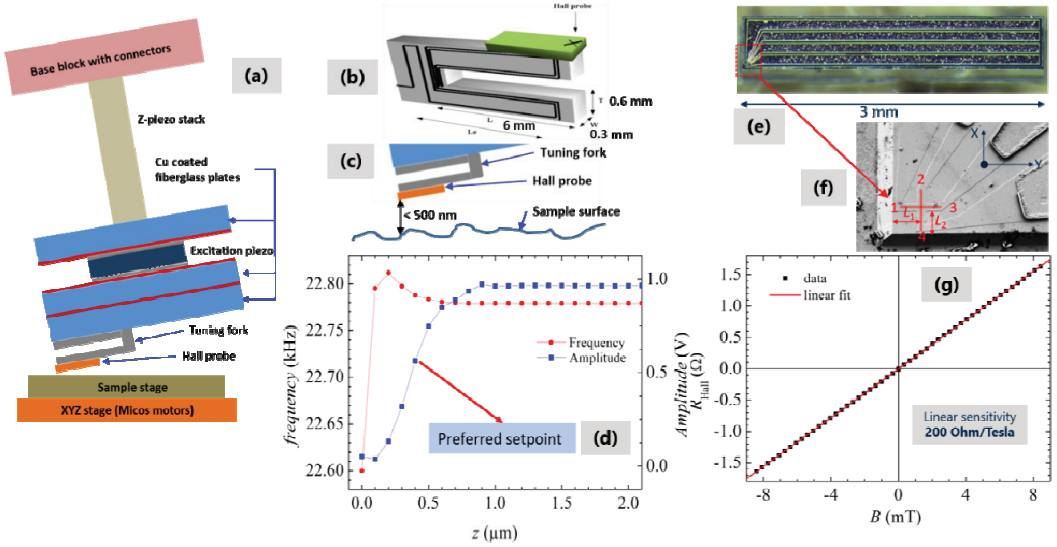

FIGURE 1. (a) Schematic of the microscope. (b) Schematic showing a Hall bar mounted on a tuning fork. (c) Typical probe-sample contact regulation during a scan. (d) Approach curve of a tuning fork with a probe mounted on it. Note the reduced f_R, due to anchoring of one prong of the tuning fork to the probe plate, and the Hall probe mounted on the other prong. (e) Optical image of a Hall bar. (f) SEM image of the Hall bar showing the Hall cross. (g) Calibration curve of a Hall sensor. The graph shows B vs. R_{Hall} data, along with linear fit of the data.

Probe-Sample Distance Regulation

Real-time control of the probe-sample distance (h) is crucial in a scanning probe setup to approach the probe close to the sample without crashing it, e.g., as in the schematic shown in Fig. 1(c). This is achieved by regulating the extension of the z-piezo stack during a scan via a PID control using the amplitude of oscillation of the tuning fork for feedback [14] to maintain a desired h. The basis of the regulation is that the amplitude of oscillation of the tuning fork decreases monotonically on approaching the sample surface (cf. Fig. 1(d)). Typically, a desired setpoint for h is chosen, and the amplitude of oscillation of the tuning fork is regulated accordingly, e.g., to set $h \sim 500$ nm, the amplitude od oscillation is regulated at ~ 50% of the value when the tuning fork is far from the sample surface, as shown in Fig. 1(d).

Magnetic Field Detection

The Hall probes consist of heterostructures of GaAs/AlGaAs two-dimensional electron gas (2DEG) materials. Figure 1(e) shows an optical image of a typical Hall bar. Figure 1(f) shows an SEM image of a portion of the Hall

bar showing the Hall cross (identified by the red lines) and contact leads. The four edges of the Hall cross are labelled as 1, 2, 3, and 4. The distances of the Hall cross from the edges of the Hall bar are shown as L_1 and L_2 (typically 8-15 μm). Hall probes of size 1-5 μm have been prepared. See Ref. 10 for further details on the preparation and properties of the Hall probes. A typical calibration curve for the Hall probes is shown in Fig. 1(g), which shows a clear linear variation of the Hall resistance (R_{Hall}) with magnetic field (B). The Hall sensitivity (k) is determined to be ~ 200 ± 2 Ω/T for all probes used in our microscope.

To protect the probe from damage due to brushing against the sample surface, the probe is kept at a slight tilt with respect to the sample stage during a scan. The effective distance of the probe from sample surface during a scan can be estimated by taking into account the distance of the Hall cross from the Hall bar edges (L_1 and L_2), and the tilt angles along the x and y axes (cf. Ref. 10 for detailed calculations). A minimum effective probe-sample distance < 2 μm has been achieved in our microscope

Further, scanning at any desired height above the sample surface, within a z-range of 35 mm, is also possible. Apart from scanning measurements, the system has also been extensively used for fast recording of local $B(z)$ profiles.

MEASUREMENTS

The microscope has been extensively used for characterization of a wide range of magnetic structures: hard and soft magnetic materials, topographically as well as thermomagnetically patterned micro-magnetic structures, and commercial bulk permanent magnets [10,15-17]. Discussed below are a few results highlighting the high resolution and long-range scanning capabilities of the microscope.

Topographically Patterned NdFeB Micro-Pillar Array

Figures 2(c)–2(h) show a set of SHPM images showing the z-component of the stray field (B_z) over a 200 μm × 200 μm area in a 2D array of topographically patterned NdFeB micro-pillars embedded in PDMS (polydimethylsiloxane) at different scan heights. The scan resolution is 1 μm. A schematic of the sample in Fig. 2(a) shows the relevant feature sizes. The topographic image in Fig. 2(b), obtained simultaneously with the SHPM image obtained closest to the sample surface, clearly shows the modulations in the PDMS due to the underlying micro-pillars. From Figs. 2(c)–2(h), large field variation due to the micro-pillars, with B_z varying between ~ 28 mT at their centers, and ~ - 11 mT in between them, is observed at the nearest scan height h ~ 10 μm. With increasing h, the B_z variations diminish. At h ~ 70 μm, the variations disappear altogether, and B_z ~ 0 is measured across the image area.

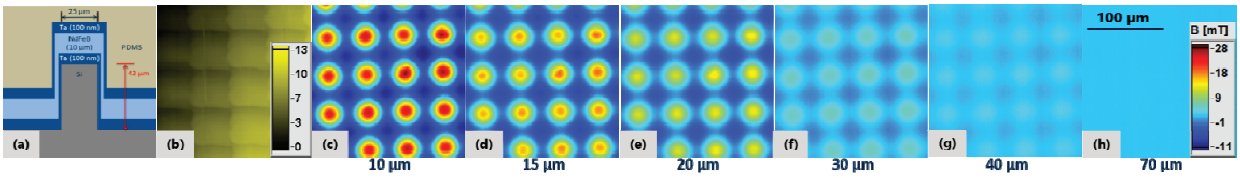

FIGURE 2. (a) Schematic of a micro-pillar in the NdFeB micro-pillar array embedded in PDMS sample. (b) Image showing topography of the sample (the scale bar is in μm). (c)-(h) SHPM images showing the B_z distribution over the sample at different scan heights, as indicated. The B_z distribution in these images is represented by the common scale bar shown in (h).

Imaging Large Magnetic Structures

Figure 3(a) shows a sample consisting of arrays of square and circular dots of 1 mm side/diameter consisting of carbonyl-iron powder mixed with PDMS embedded in a pure PDMS matrix (sample A), placed on top of a 5 mm cubic magnet. Figures 3(b)–3(c) show SHPM images showing the B_z distribution over a 2 mm × 2 mm area and at a scan height of ~ 60 μm, across a square and circular dot, respectively. The scan resolution is 5 μm. The strong concentration of flux emanating from the underlying magnet by the dots is clear from these images. Figures 3(d)–3(e) show SHPM images of a sample consisting of NdFeB dots of similar dimensions (sample B). From these images, we can readily observe the variation of magnetic flux across the dots, with flux strongly concentrated near the edges, and decreasing towards the centers of the dots.

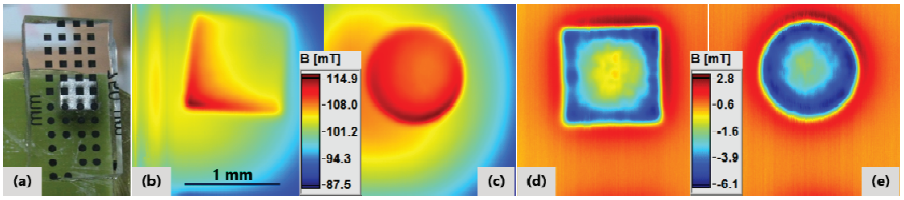

FIGURE 3. (a) Sample A placed on top of a 5 mm cubic magnet. (b)-(c) SHPM images showing the B_z distribution in sample A at a scan height of 60 µm. The scale bar in between represents B_z variation in both images. (d)-(e) SHPM images showing the B_z distribution in sample B at a scan height of 60 µm. The scale bar in between represents B_z variation in both images.

In summary, we have developed a scanning Hall probe microscope for high resolution, large area, variable height magnetic field imaging, for the quantitative characterization of micro-magnets as well as mm-sized magnetic structures.

ACKNOWLEDGMENTS

The authors sincerely thank D. Le Roy, T. Devillers, D. Givord (Institut Néel), and Marie Frénéa-Robin (Laboratoire Ampère, Lyon) for providing samples and for fruitful discussions. This work was partially funded by the ANR "MIME" Project (No. ANR-11-BSV5-0101). The work of R. B. G. K. is partially supported by the "Chaire Initiative Universitaire Alpes (IUA)" of the University Grenoble Alpes. G. S. would like to thank the electronics workshop at Institut Néel for technical support, and S. Le-Denmat and S. Samaddar for their inputs. The authors acknowledge the contributions of D. J. Hykel, M. Kustov, and P. Laczkowski in development of an earlier generation of the microscope. The 2DEG wafers used for sensor fabrication were provided by Picogiga (Soitec). Probes were patterned at the Nanofab cleanroom facility of Institut Néel.

REFERENCES

1. A. M. Chang, H. D. Hallen, L. Harriott, H. F. Hess, H. L. Kao, J. Kwo, R. E. Miller, R. Wolfe, J. van der Ziel, and T. Y. Chang, Appl. Phys. Lett. **61**, 1974 (1992).
2. A. Oral, S. J. Bending, and M. Henini, Appl. Phys. Lett. **69**, 1324 (1996).
3. A. Sandhu, H. Masuda, A. Oral, S. Bending, A. Yamada, and M. Konagai, Ultramicroscopy **91**, 97–101 (2002).
4. J. K. Gregory, S. J. Bending, and A. Sandhu, Rev. Sci. Instrum. **73**, 3515 (2002).
5. R. B. Dinner, M. R. Beasley, and K. A. Moler, Rev. Sci. Instrum. **76**, 103702 (2005).
6. V. Cambel, J. Fedor, D. Greguov, P. Kov, and I. Huek, Supercond. Sci. Technol. **18**, 417–421 (2005).
7. C.-C. Tang, H.-T. Lin, S.-L. Wu, T.-J. Chen, M. J. Wang, D. C. Ling, C. C. Chi, and J.-C. Chen, Rev. Sci. Instrum. **85**, 083707 (2014).
8. Ö. Karcı, J. O. Piatek, P. Jorba, M. Dede, H. M. Rønnow, and A. Oral, Rev. Sci. Instrum. **85**, 103703 (2014).
9. M. Shimizu, E. Saitoh, H. Miyajima, and H. Masuda, J. Magn. Magn. Mater. **282**, 369–372 (2004).
10. G. Shaw, R. B. G. Kramer, N. M. Dempsey, and K. Hasselbach, Rev. Sci. Instrum. **87**, 113702 (2016).
11. M. Kustov, P. Laczkowski, D. Hykel, K. Hasselbach, F. Dumas-Bouchiat, D. O'Brien, P. Kauffmann, R. Grechishkin, D. Givord, G. Reyne, O. Cugat, and N. M. Dempsey, J. Appl. Phys. **108**, 063914 (2010).
12. C. Veauvy, K. Hasselbach, and D. Mailly, Rev. Sci. Instrum. **73**, 3825–3830 (2002).
13. D. J. Hykel, Z. S. Wang, P. Castellazzi, T. Crozes, G. Shaw, K. Schuster, and Hasselbach, J. Low Temp. Phys. **175**, 861–867 (2014).
14. K. Karrai and R. D. Grober, Appl. Phys. Lett. **66**, 1842 (1995).
15. N. M. Dempsey, D. Le Roy, H. Marelli-Mathevon, G. Shaw, A. Dias, R. B. G. Kramer, M. Kustov, L. F. Zanini, C. Villard, K. Hasselbach, C. Tomba, and F. Dumas-Bouchiat, Appl. Phys. Lett. **104**, 262401 (2014).
16. D. Le Roy, G. Shaw, R. Haettel, K. Hasselbach, F. Dumas-Bouchiat, D. Givord, and N. M. Dempsey, Mater. Today Commun. **6**, 50 (2016).
17. D. Mitrossilis, J. Röper, D. Leroy, B. Driquez, A. Michel, C. Ménager, G. Shaw, S. Le Denmat, L. Ranno, F. Dumas-Bouchiat, N. M. Dempsey, and E. Farge, Nature Communications **8**, 13883 (2017).